



HAL
open science

“Click” Chemistry for the Functionalization of Graphene Oxide with Phosphorus Dendrons: Synthesis, Characterization and Preliminary Biological Properties

Omar Alami, Regis Laurent, Marine Tassé, Yannick Coppel, Jérôme Bignon, Saïd El Kazzouli, Jean-pierre Majoral, Nabil El Brahmi, Anne-marie Caminade

► To cite this version:

Omar Alami, Regis Laurent, Marine Tassé, Yannick Coppel, Jérôme Bignon, et al.. “Click” Chemistry for the Functionalization of Graphene Oxide with Phosphorus Dendrons: Synthesis, Characterization and Preliminary Biological Properties. *Chemistry - A European Journal*, 2023, 29 (66), pp.e202302198. 10.1002/chem.202302198 . hal-04269848

HAL Id: hal-04269848

<https://hal.science/hal-04269848>

Submitted on 3 Nov 2023

HAL is a multi-disciplinary open access archive for the deposit and dissemination of scientific research documents, whether they are published or not. The documents may come from teaching and research institutions in France or abroad, or from public or private research centers.

L'archive ouverte pluridisciplinaire **HAL**, est destinée au dépôt et à la diffusion de documents scientifiques de niveau recherche, publiés ou non, émanant des établissements d'enseignement et de recherche français ou étrangers, des laboratoires publics ou privés.

“Click” Chemistry for the Functionalization of Graphene Oxide with Phosphorus Dendrons: Synthesis, Characterization and Preliminary Biological Properties

Omar Alami,[a,b,c] Régis Laurent,[a,b] Marine Tassé,[a,b] Yannick Coppel,[a,b] Jérôme Bignon,[d] Saïd El Kazzouli,[c] Jean-Pierre Majoral,[a,b] Nabil El Brahmi*[c] and Anne-Marie Caminade*[a,b]

Dedicated to Prof. Dr. Evamarie Hey-Hawkins on the occasion of her retirement

[a] Dr O. Alami, Dr R. Laurent, M. Tassé, Dr Y. Coppel, Dr J.P. Majoral, Dr A.M. Caminade

Laboratoire de Chimie de Coordination, CNRS, 205 route de Narbonne, 31077 Toulouse Cedex 4, France. E-mail: anne-marie.caminade@lcc-toulouse.fr

[b] Dr O. Alami, Dr R. Laurent, M. Tassé, Dr Y. Coppel, Dr J.P. Majoral, Dr A.M. Caminade

LCC-CNRS, Université de Toulouse, CNRS, Toulouse, France

[c] Dr O. Alami, Prof Dr S. El Kazzouli, Prof Dr N. El Brahmi

Euromed Research Center, Euromed Faculty of Pharmacy, Euromed University of Fes (UEMF), Route de Meknes, 30000 Fez, Morocco, E-mail: n.elbrahmi@ueuromed.org

[d] Dr J. Bignon

Plateforme CIBI, ICSN, CNRS, Centre de Recherche de Gif, Bâtiment 27, 1 avenue de la Terrasse, 91198 Gif-sur-Yvette Cedex, France

Abstract: Two families of phosphorhydrazone dendrons having either an azide or an alkyne linked to the core and diverse types of pyridine derivatives as terminal functions have been synthesized and characterized. These dendrons were grafted via click reaction to graphene oxide (GO) functionalized with either alkyne or azide functions, respectively. The resulting modified-GO and GO-dendrons materials have been characterized by Fourier Transform Infrared (FTIR), Raman spectroscopy (RS), and Magic Angle Spinning Nuclear Magnetic Resonance (MAS-NMR) analyses. In addition, the free dendrons and the dendrons grafted to GO were tested toward cancerous (HCT116) and non-cancerous (RPE1) cell lines.

Introduction

“Click” chemistry was proposed by K.B. Sharpless et al. in 2001 [1] to describe reactions being simple, quantitative, easy to carry out, and for which by-products are easily removed. Among these click reactions, the cycloaddition reaction between alkynes and azides, catalyzed with copper, is one of the most widely used. Such reaction forms a 1,2,3-triazole, specifically substituted in 1,4. It is also frequently named copper(I) catalyzed azide-alkyne cycloaddition (CuAAC) reactions. Such type of [2+3] cyclization reaction was proposed previously by R. Huisgen et al. [2], but without Cu, resulting in a mixture of triazoles substituted in 1,4 and 1,5.

Besides the use of such click reaction for the synthesis of a large variety of organic compounds, in particular drugs [3], it has been also applied for the grafting of organic compounds to diverse materials. Among them is graphene oxide (GO), which is generally produced from graphite by the “Top-Down” method [4], by oxidation reactions, introducing various oxygenated functional groups. GO has been functionalized by click chemistry for diverse purposes such as catalysis [5], sensing Cu²⁺[6], biosensing [7], and biological applications [8], to name a few.

Among the compounds grafted to GO via click reactions between azides and alkynes, Sarkar et al. were the only ones to the best of our knowledge who have grafted a dendron. This compound was a PAMAM dendron, functionalized with an alkyne at the core and NH₂ groups as terminal functions, which was grafted to GO functionalized with azides, the resulting material being used for gene delivery [9]. Dendrons [10] are dendritic wedges, which can not only be considered as building blocks for the synthesis of dendrimers [11], but can also be amphiphilic and thus be able to self-associate [12]. Both dendrons and dendrimers are hyperbranched well-defined macromolecules, synthesized step-by-step by a repetitive process, which generates a new generation at each repetitive cycle [13]. As the size increases with the number of generations, it becomes rapidly difficult to draw the full structure. Thus, dendrons and dendrimers can be represented in a linear form, with parentheses at each generation, and a number indicating the multiplication of the branches (Figure 1). The main difference between dendrons and dendrimers is the presence of a single function at the core of dendrons but not of dendrimers. The presence of such single function at the core of dendrons is particularly useful for their grafting to materials.

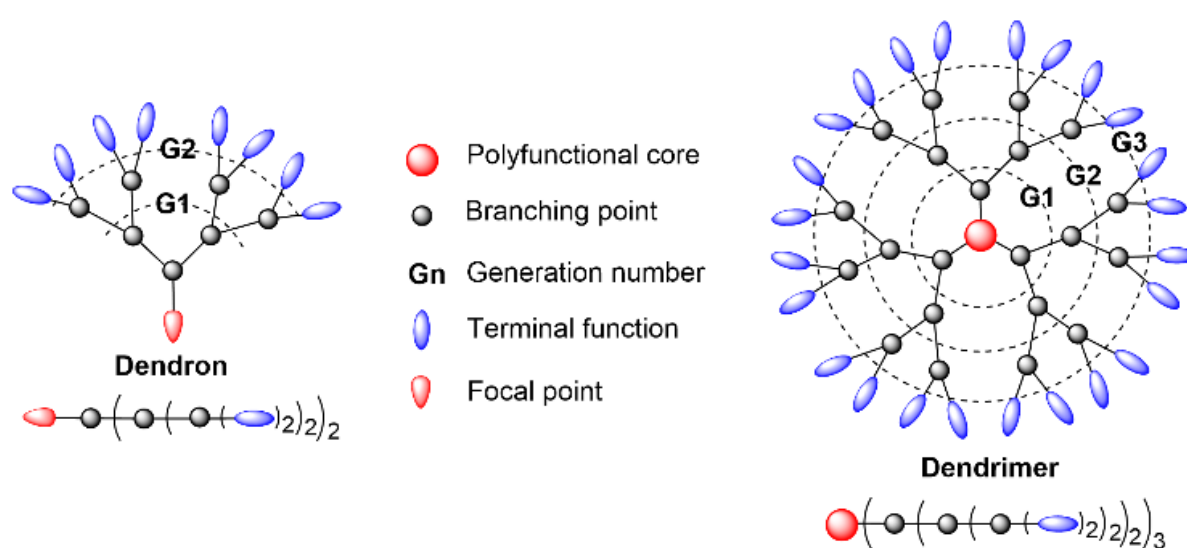


Figure 1. Schematized structure of a dendron and a dendrimer, represented both as the full structure and in linear form.

Among the diverse types of dendrimers and dendrons, those built with phosphorhydrazone linkages [14] display interesting properties in many fields [15] such as the elaboration of special dendritic architectures [16], catalysis [17], fluorescence [18], nanomaterials [19], biomaterials [20], and biology/nanomedicine [21]. A particular series of phosphorhydrazone dendrimers bearing pyridine derivatives as terminal functions, either free or complexing diverse metals such as copper [22] or gold [23], have displayed potent anti-cancer properties [24]. Amphiphilic dendrons bearing the same types of complexes as terminal functions have also displayed anti-cancer properties [25].

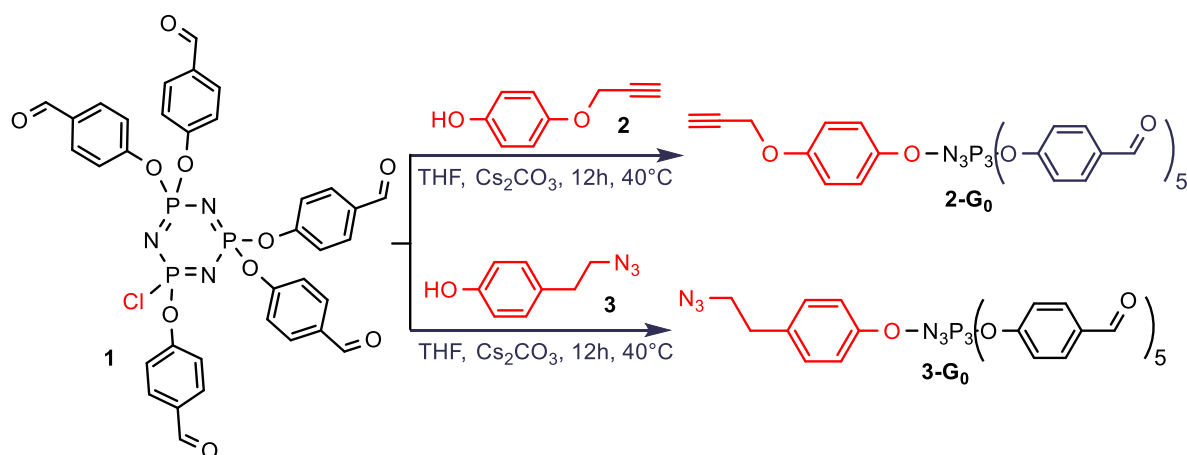
In view of the numerous biological properties of GO in oncology [26], used for instance for theranostic [27], for imaging [28], and for drug delivery [29], it appeared tempting to graft phosphorhydrazone dendrons bearing pyridine derivatives as terminal functions to GO, as will be shown below. As indicated in the first part of the introduction, the CuAAC reactions are particularly efficient and versatile, thus we applied them for grafting the dendrons to GO. For this purpose, GO was functionalized with either azides or alkynes, whereas a single function at the core of dendrons was either an alkyne or an azide. The surface of the dendrons was functionalized with diverse types of pyridine derivatives which can display anti-cancer properties either complexing metals such as copper or gold, but also free [22]. It

was expected that gathering together many active functions on the surface of GO could increase their anti-cancer efficiency.

Results and Discussion

Synthesis and characterization of dendrons

The synthesis of the phosphorhydrazone dendrons is based on the selective functionalization of hexachlorocyclotriphosphazene (N₃P₃Cl₆) with one function different from the five others [30]. In the first step, five equivalents of 4-hydroxybenzaldehyde were grafted to N₃P₃Cl₆, affording the pentaaldehyde **1** [31]. The second step concerned the synthesis of phenols suitably functionalized for click chemistry, i.e. with either an alkyne or an azide. Phenol **2** was obtained from the reaction of hydroquinone with propargyl bromide [32]. Phenol **3** was synthesized in two steps, first the reaction of 2-(4-hydroxyphenyl)ethanol in HBr at 85 °C [33], then the conversion of bromine to azide with NaN₃ in DMF [34]. Having in hand both types of precursors, the functionalized phenols **2** and **3** were reacted with the pentaaldehyde **1** (Scheme 1). Compounds **2-G0** and **3-G0** were isolated in 43% and 78% yield, respectively, after purification by column chromatography.



Scheme 1. Synthesis of generation 0 of the dendrons functionalized with either an alkyne (**2-G0**) or an azide (**3-G0**) at the core.

The characterization by ³¹P NMR spectroscopy displays a singlet for **3-G0**, but a complex spectrum for **2-G0**, due to the magnetic non-equivalence of the phosphorus atoms of the cyclotriphosphazene. However, simulation of the AB₂ system expected for such type of compound do confirm its purity, and affords the chemical shift values of A at 8.23 ppm and of B at 7.57 ppm, with a JPP coupling constant of 91.2 Hz (Figure 2). The different ³¹P NMR behavior of compounds **2-G0** and **3-G0** is probably due to the nature of the atom in para position in the phenoxy groups. The six phenoxy groups have a carbon atom in para position for compound **3-G0**, and all of them are viewed as equivalent by ³¹P NMR. On the contrary, one of the phenoxy group has an oxygen atom in para position for compound **2-G0**. This substituent is viewed as different from the five others by ³¹P NMR, which could explain the presence of an AB₂ system only in this case.

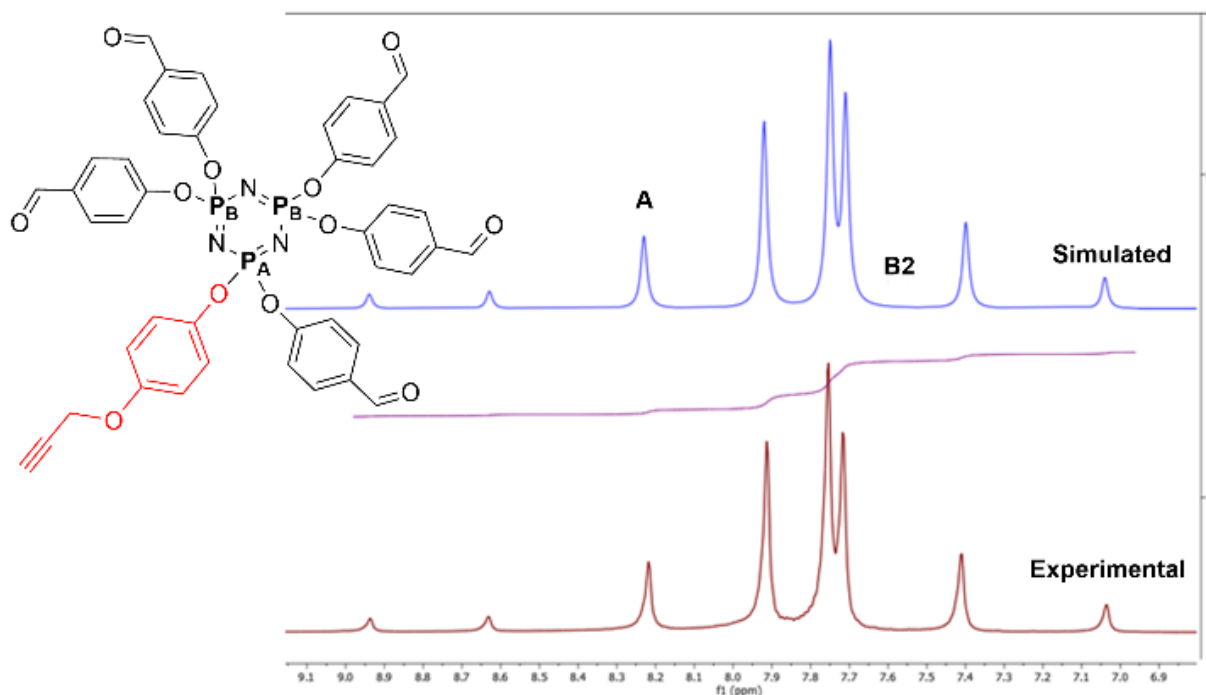
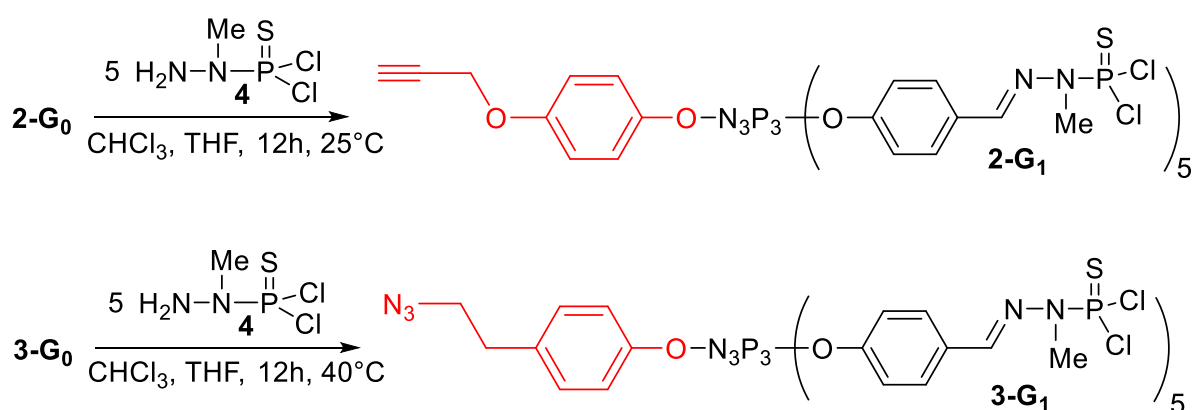


Figure 2. Experimental and simulated $^{31}\text{P}\{^1\text{H}\}$ NMR spectra of 2-G0.

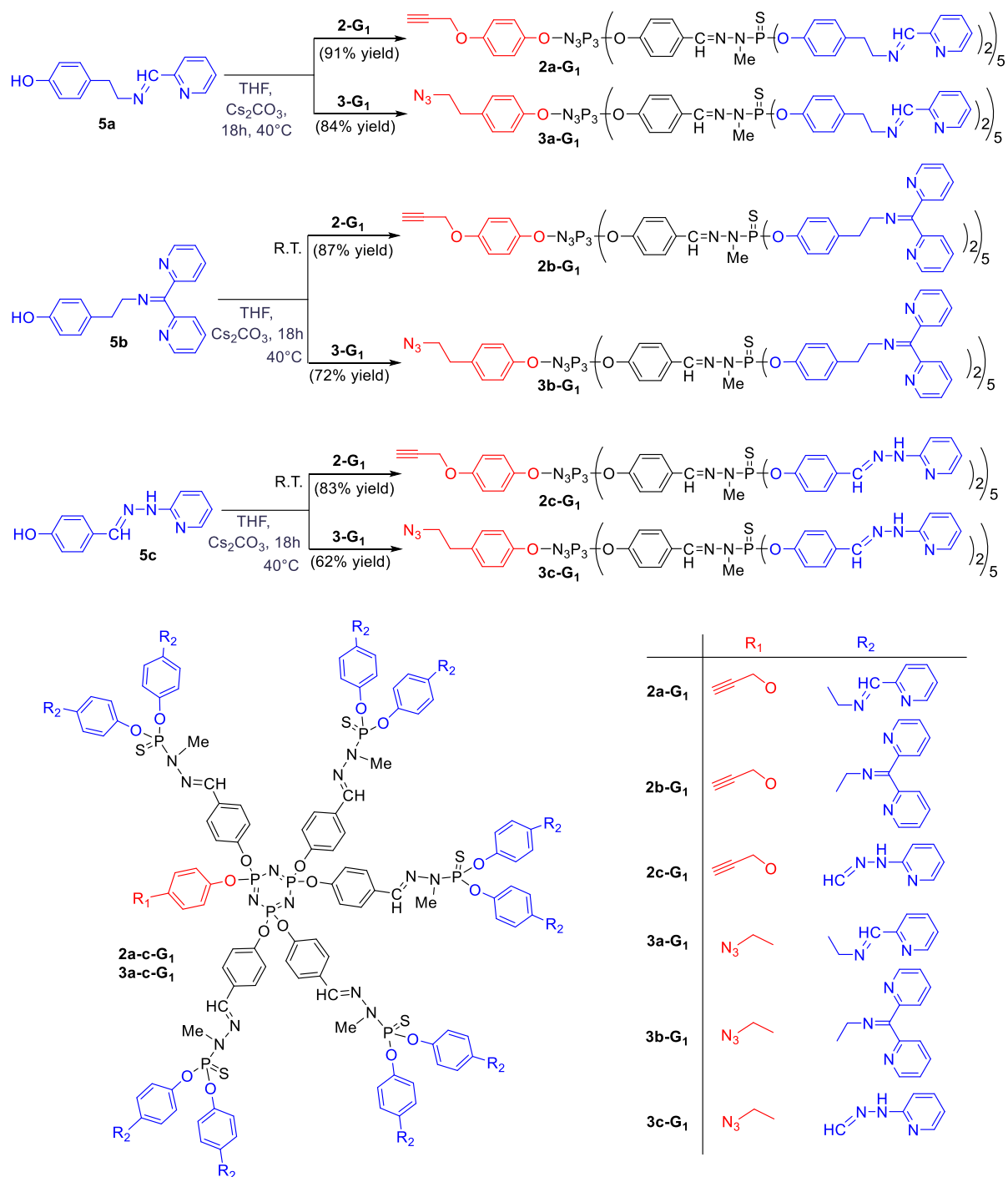
The growing of the dendrons was then carried out by condensation reaction between the aldehydes and the dichlorothiophosphorhydrazide **4**, obtained by reaction of methylhydrazine with $\text{P}(\text{S})\text{Cl}_3$ at $-60\text{ }^\circ\text{C}$. The condensation reaction was monitored by the disappearance of the signal of the aldehyde groups in ^1H NMR. Dendrons 2-G1 and 3-G1 (Scheme 2) were isolated in 89% and 84% yield, respectively. ^{31}P NMR is again very informative of the structure of the dendrons. Indeed, three signals in a 2:1:2 ratio were observed for the five $\text{P}(\text{S})\text{Cl}_2$ terminal functions of dendron 2-G1. Such behavior is an illustration of the presence of two $\text{P}(\text{S})\text{Cl}_2$ groups above the plane defined by N_3P_3 , two below, and one $\text{P}(\text{S})\text{Cl}_2$ group opposite to the phenol alkyne. In the case of 3-G1, two signals are observed for the five $\text{P}(\text{S})\text{Cl}_2$ terminal functions in a 3:2 ratio, for the same reason, as previously reported for another dendron [35].



Scheme 2. Synthesis of the first generation of dendrons 2-G1 and 3-G1.

The synthesis of the dendrons could be carried out up to the second or third generation, but we decided to stop the growing at the first generation to preserve the accessibility of the function linked to the core. Indeed, we have previously demonstrated that only the first generation dendrons bearing the thioctic acid at the core (instead of the alkyne or azide) could be grafted to a gold surface, not the

second generation, for which the core was not enough accessible [36]. The last step of the synthesis of the dendrons was the decoration of their surface with diverse phenol-pyridine derivatives. These compounds were synthesized as previously described by condensation reactions of tyramine with 2-pyridine carboxaldehyde or di(2-pyridyl) ketone, affording compounds 5a and 5b, respectively [37]. Compound 5c was obtained by condensation reaction of 4-hydroxybenzaldehyde with 2-hydrazinopyridine [22a]. Compounds 5a-c were then reacted in basic conditions with the first generation dendrons 2-G1 and 3-G1, to afford dendrons 2a-c-G1 and 3a-c-G1 isolated with a yield range of 62-91% (Scheme 3).



Scheme 3. Functionalization of dendrons with phenol-pyridine derivatives, and full structure of all dendrons.

All dendrons are in particular characterized by ^{31}P NMR, which displays generally two singlets in a 2:3 ratio for the P(S)(OAr) $_2$ groups. The ^{31}P { ^1H } NMR spectrum of dendron 3a-G $_1$ is shown in Figure 3, together with the chemical structure showing 3 P=S groups up and 2 P=S groups down, relative to the cyclotriphosphazene ring. The family of dendrons 3a-c-G $_1$ is also characterized by IR, which displays the vibration corresponding to the azide group at 2100 cm^{-1} .

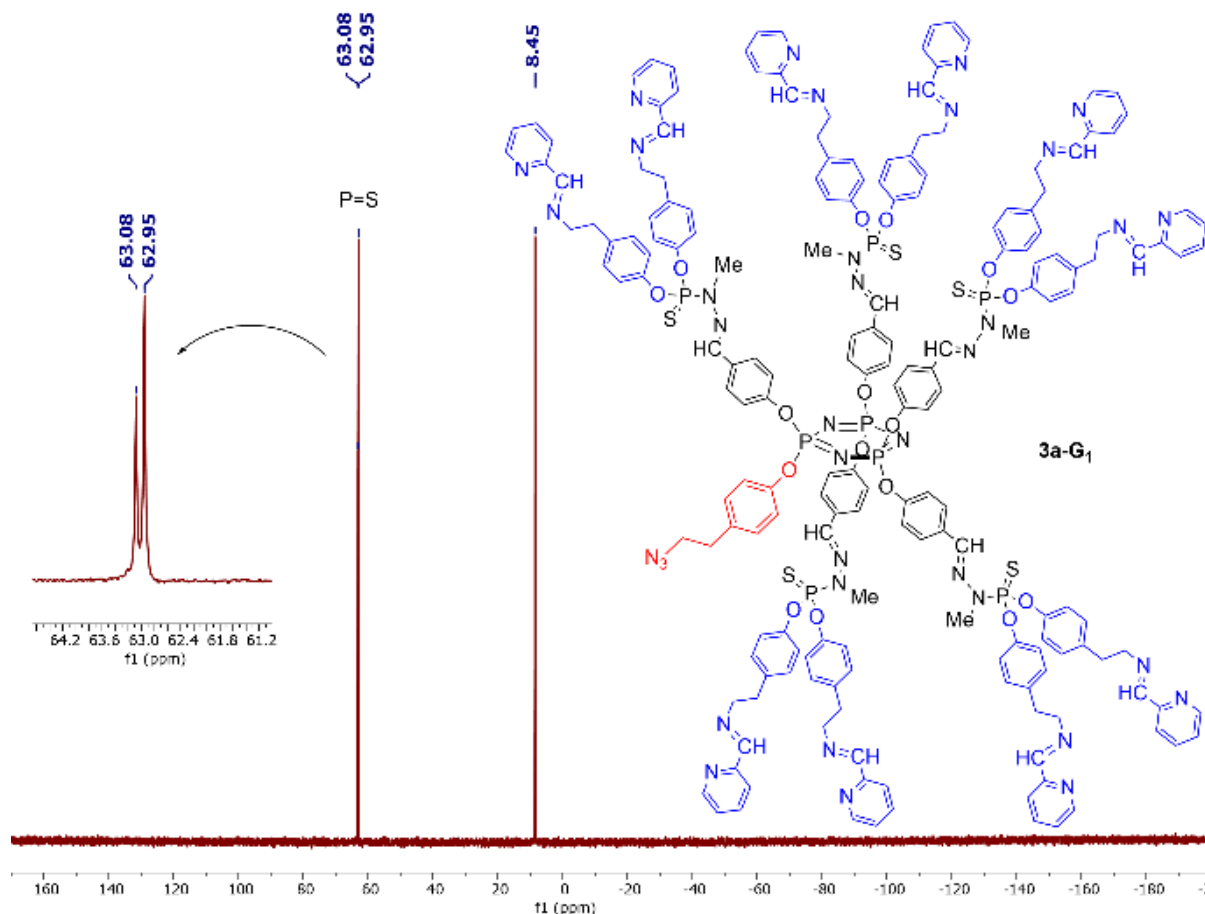


Figure 3. ^{31}P { ^1H } NMR spectrum of dendron 3a-G $_1$, with the 2 signals in the insert corresponding to the P=S groups in a 2:3 ratio, and its full chemical structure.

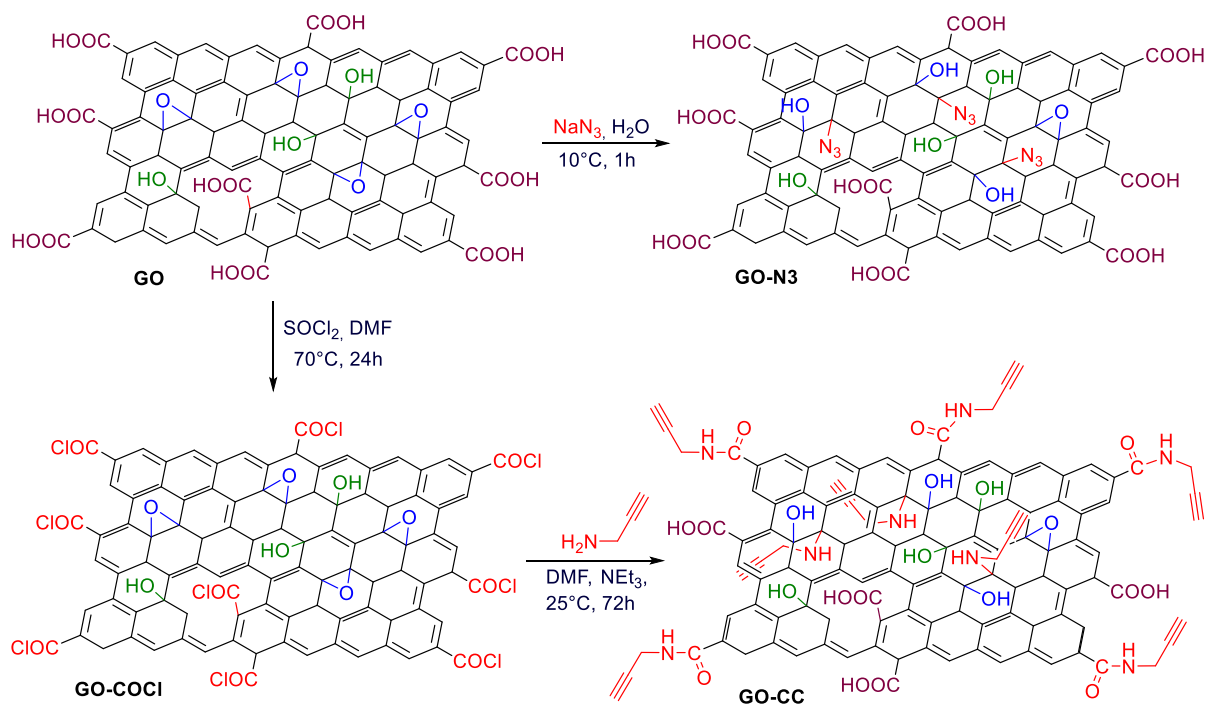
Synthesis and characterization of modified GO

GO is obtained from graphite using the Hummers method to generate first the graphite oxide [38]. This method concerns the successive addition of H_2SO_4 , NaNO_3 , and KMnO_4 to graphite. The graphite oxide obtained in this way can be exfoliated into individual GO nanosheets via the sonication approach in organic solvents such as *N,N*-dimethylformamide (DMF) and tetrahydrofuran (THF), to afford the desired GO [39].

In order to have GO suitably functionalized to be used in click reactions, it is necessary to modify some of its functions. In the first step, the azide groups were obtained by reaction of GO with sodium azide at 10 °C in water, following a published procedure [40] to generate GO-N $_3$, by opening of the epoxide rings (Scheme 4). This material is in particular characterized by IR, which displays the presence of the azide vibration at 2100 cm^{-1} , and by elementary analysis, which shows a small increase of the nitrogen content, from 0.05% for GO to 1.19% for GO-N $_3$.

The grafting of the second type of functions, the alkyne groups, was carried out in two steps from GO. The first step is the transformation of carboxylic acid to carbonyl chloride, using SOCl_2 , to afford GO-

COCl. This material is highly sensitive to hydrolysis, and was not characterized, but directly reacted with propargylamine to afford GO-CC (Scheme 4). The presence of propargylamide bonds vibration (C=O) at 1661 cm⁻¹ in IR spectra indicated that the grafting of propargylamine occurred on the carbonyl chloride. However, in view of the quite large increase of the nitrogen content found in elemental analyses (4.49%), it can be inferred that the grafting occurred also on the epoxides, as illustrated in Scheme 4.



Scheme 4. Illustration of the synthesis of GO functionalized with azide (GO-N₃) or with alkyne (GO-CC).

Raman spectra (RS) display bands corresponding to non-polar but polarizable bonds, such as C=C bonds. This technique can be used for the characterization of GO. As shown in Figure 4 the RS of GO displays three main signals at 1340 cm⁻¹ (signal D, C-C), 1580 cm⁻¹ (signal G, C=C) and 2700 cm⁻¹ (signal 2D, corresponding to layer stacking). The intensity of signal D is modified when introducing defects, such as structural defects, or hybridization modified from sp² to sp³, when grafting substituents [41]. Thus, by comparing the intensity ratio of D and G bands (I_D/I_G) of the starting material with that after reaction, it is possible to say if there is a surface modification or not. The I_D/I_G values of GO-N₃ (0.81) is comparable to I_D/I_G values of GO (0.80), however, the I_D/I_G values of GO-CC was increased up to 1.16. Both obtained results indicate a higher level of disorder and more defects on account of propargylamine groups compared to N₃ onto the GO surface. These results also confirmed the results obtained by elementary analysis.

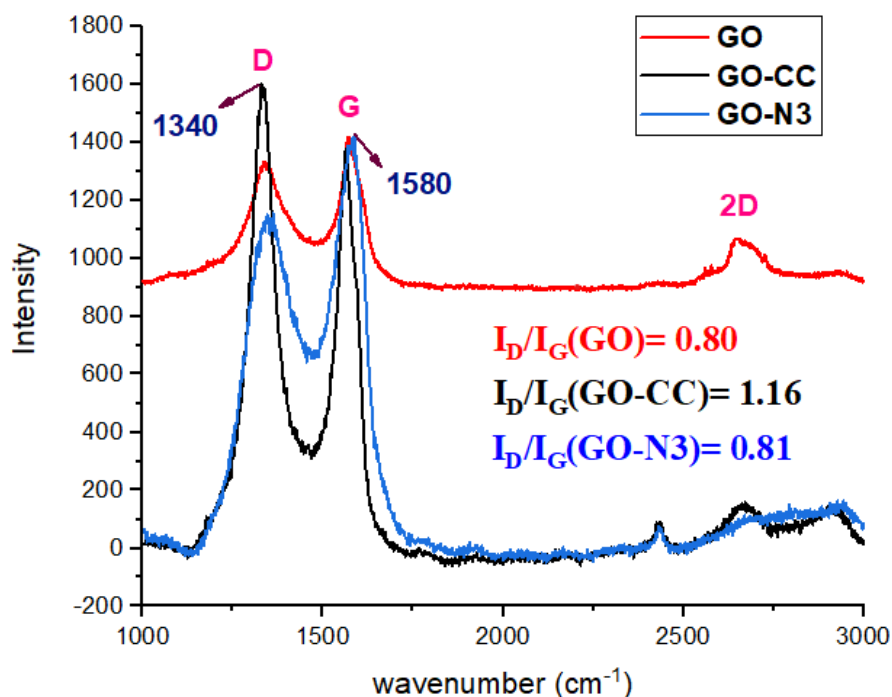
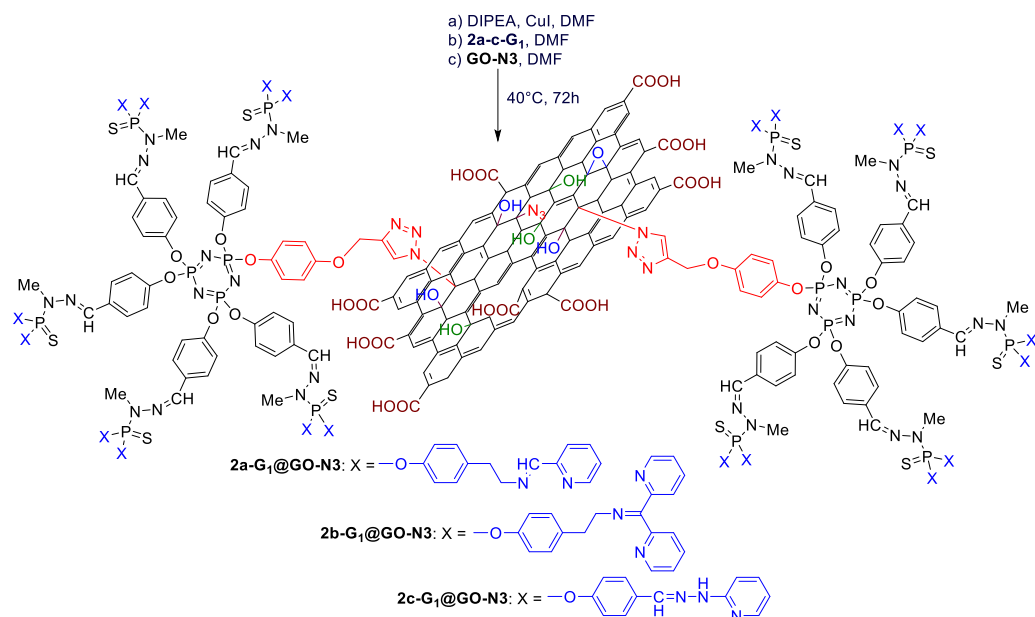


Figure 4. Raman spectra of GO, GO-N3 and GO-CC, and comparison of their ID/IG ratios.

Grafting dendrons to modified GO

Having in hand the functionalized graphene oxides GO-N3 and GO-CC, the next step was the grafting of the suitably functionalized dendrons 2a-c-G1 and 3a-c-G1, respectively. In both cases, the grafting was carried out by mixing firstly CuI and diisopropylethylamine (DIPEA) in DMF. For the series of dendrons having an alkyne at the core, a solution of dendron 2a-c-G1 in DMF, and finally a suspension of GO-N3 in DMF were added. The reaction was accomplished using the same weight of dendron and modified GO. The resulting mixture was then heated at 40 °C for 72 h, affording the functionalized graphene oxide 2a-c-G1@GO-N3 (Scheme 5).



Scheme 5. Click reaction between dendrons 2a-c-G1 and GO-N3, affording the materials 2a-c-G1@GO-N3.

Several washings were carried out with THF, MeOH, EtOH, and dichloromethane to eliminate the eventually non-grafted dendrons, then the black solids of 2a-c-G1@GO-N3 were dried under vacuum. Different techniques were used for characterizing the presence of the dendrons linked to GO-N3. ³¹P MAS NMR displays the presence of two signals at about 8 and 62 ppm, corresponding to the N3P3 core, and P(S)X2 terminal functions, respectively, as illustrated for 2b-G1@GO-N3 (Figure 5A). Raman spectroscopy is very informative of the grafting of dendrons, with an important modification of the ID/IG ratios. It should be noted that in this case, the reaction transforming the azide to a triazole occurs very close to the surface of GO, and thus this can explain the modification of the ID/IG ratios. The obtained ID/IG ratios for 2a-G1@GO-N3, 2b-G1@GO-N3 and 2c-G1@GO-N3 are 1.10, 1.02 and 1.20, respectively. These values, albeit heterogeneous, are comparable to the value obtained in the case of the reaction of GO with propargylamine (1.17). All these results do confirm the covalent grafting of the different dendrons on GO-N3 via click reaction (Figure 5B).

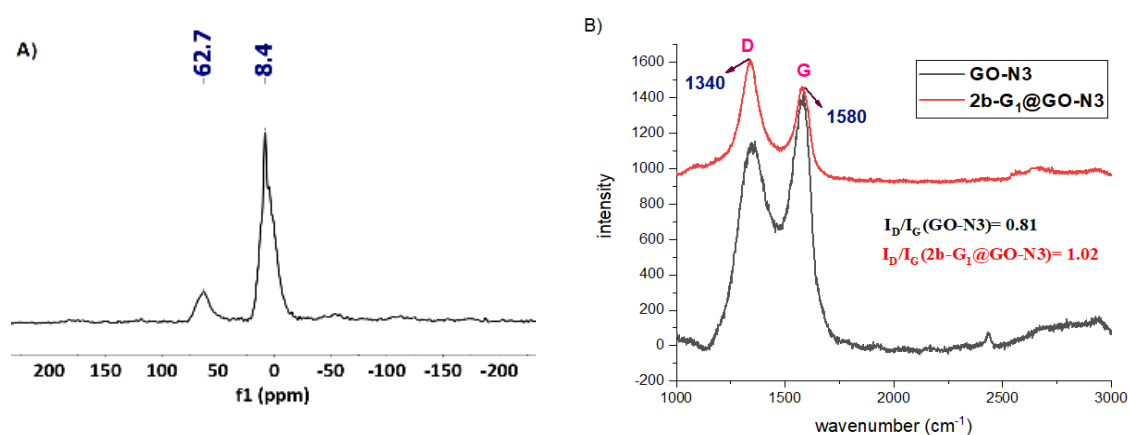


Figure 5. Characterization of material 2b-G1@GO-N3. A) ³¹P MAS NMR of 2b-G1@GO-N3. B) Raman spectra of GO-N3 (black) and 2b-G1@GO-N3 (red).

IR spectra confirm the grafting of the dendrons, as shown by the comparison between GO-N3, dendron 2b-G1, and 2b-G1@GO-N3 (Figure 6). The spectrum of the material functionalized with the dendron displays clearly the fingerprint of the dendron, confirming the grafting. However, not all the azides have reacted, as shown by the presence of a very small azide vibration at 2100 cm⁻¹.

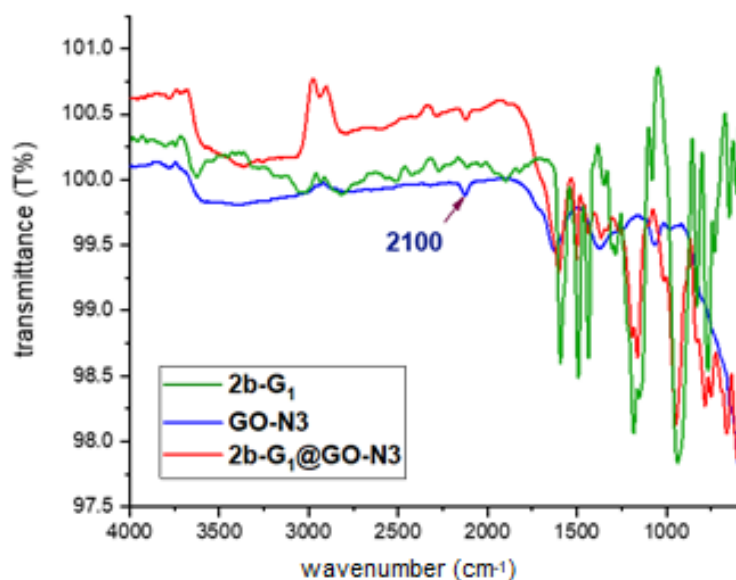
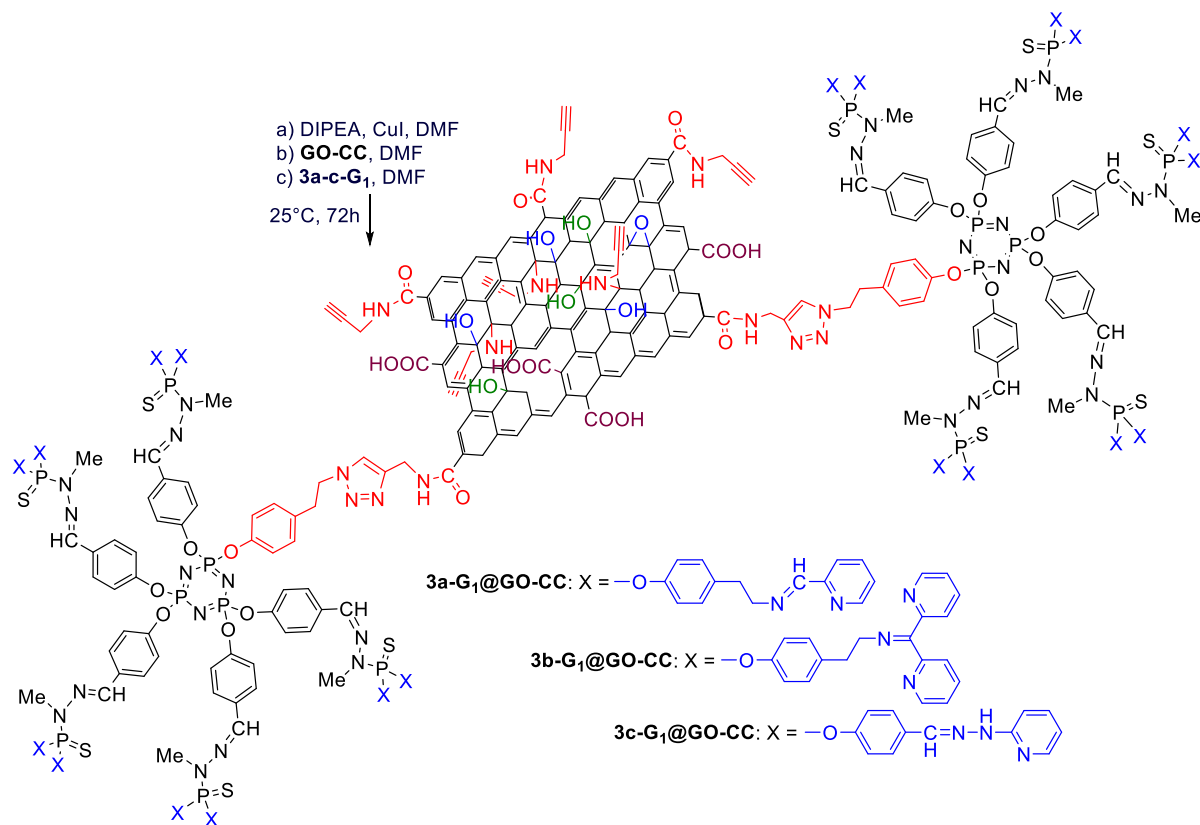


Figure 6. IR spectra of GO-N3 (blue), dendron 2b-G1 (green), and 2b-G1@GO-N3 (red).

The second series of dendrons (3a-c-G1) was used to react with the material GO-CC. In that case, after mixing CuI and diisopropylethylamine in DMF, a suspension of GO-CC in DMF and finally dendrons 3a-c-G1 were added, and the mixture was stirred at 40 °C for 72 h (Scheme 6). As in the previous case, several washings with the same solvents were carried out to eliminate the eventually non-grafted dendrons.



Scheme 6. Click reaction between dendrons 3a-c-G1 and GO-CC, affording the materials 3a-c-G1@GO-CC.

The absence of signal at 2100 cm⁻¹ for the azide in the IR spectra of the materials 3a-c-G1@GO-CC confirmed the efficiency of the washings. ³¹P MAS NMR displays the presence of two signals at about 8 and 62 ppm, as for the previous series, confirming the grafting of the dendrons. Raman spectroscopy of this family (Figure 7) displayed a slight modification of the ID/IG ratios between GO-CC (1.16) and 3a-G1@GO-CC (1.20). As in that case the reactions occur relatively far from the GO surface, no large variation of the ID/IG ratios were expected. Nevertheless, when grafting 3b-G1 and 3c-G1 dendrons to GO-CC, the intensity ratio of D over G band of 3b-G1@GO-CC (1.10) and 3c-G1@GO-CC (1.00) are lower than that of GO-CC (1.16), but display the same range of heterogeneity, as observed with 2a-c-G1@GO-N3. The observed decrease of the ID/IG ratios might be related in part to a reversed transformation of the amino alcohols to the epoxides on the surface of the graphene oxide. Indeed, there are many publications describing amino alcohols as precursors of cyclic ethers, including of epoxides, in the presence of either acids or bases [42]. The use of DIPEA may facilitate such reverse reaction, which should decrease the disorder on the surface of GO, and thus decreases the ID/IG ratios, but may also decrease the efficiency of the grafting of these dendrons.

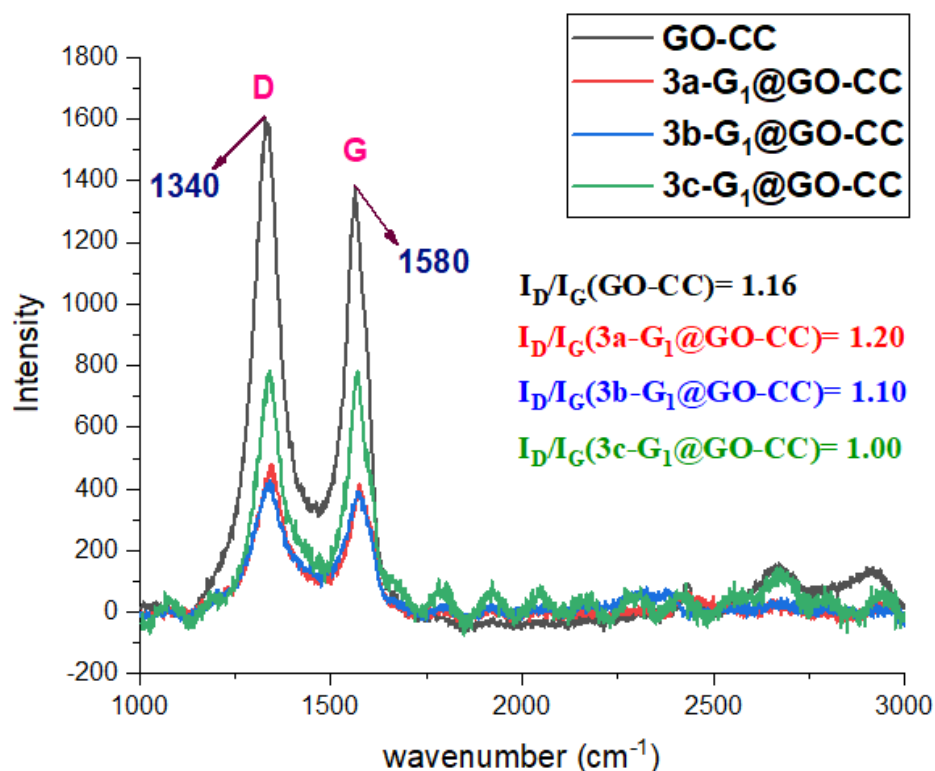


Figure 7. Raman spectra of GO-CC (black), 3a-G₁@GO-CC (red), 3b-G₁@GO-CC (blue) and 3c-G₁@GO-CC (green).

In order to quantify the efficiency of the grafting of dendrons to GO, elemental analyses were carried out on sulfur, as this element is exclusively present in the dendrons. As the same weight of dendron and GO has been used in all cases, the theoretical percentage of sulfur can be easily calculated. Comparison with the measured S% affords a direct access to the efficiency of the grafting (Table 1). It is clear from these data that a substantial quantity of dendrons was grafted in all cases, but the first type of grafting (GO functionalized with azides) is more efficient than the second one (GO functionalized with alkyne). Besides, it can be noted that there is a clear correlation between the efficiency of the grafting determined by elemental analyses and the Raman data, in particular considering the case of materials 3b-G₁@GO-CC and 3c-G₁@GO-CC, which have the lower percentage of grafting.

The results obtained with sulfur seem contra-intuitive when considering the larger increase in N content in GO-CC compared to GO-N3. However, due to their size, the dendrons are able to screen a part of the GO surface, and thus an increase in the number of reactive sites cannot guaranty an increase of the quantity of dendrons grafted. Besides, the environment of the azide at the core of the dendrons or on the surface of GO-N3 is quite similar, whereas the environment of the alkyne is quite different. The alkyne is grafted to the dendron through a CH₂-O-Ar linker, whereas it is grafted to GO through a CH₂-NH-C=O linker. It is well-known that amide linkages can associate by hydrogen bonding, which may occur between different GO-CC sheets, decreasing its ability to react with the dendrons, due to the steric hindrance.

Table 1. Elemental analyses of the sulfur content in the materials

Dendrons@GO	Theoretical S%	Measured S% ^[a]	% of dendron grafted	Mol% of dendron per g of materials
2a-G1@GO-N3	2.23	1.69	76	1.20 10 ⁻⁴
2b-G1@GO-N3	1.83	1.49	81	1.03 10 ⁻⁴
2c-G1@GO-N3	2.31	2.30	99	1.73 10 ⁻⁴
3a-G1@GO-CC	2.22	1.66	75	1.19 10 ⁻⁴
3b-G1@GO-CC	1.83	0.88	48	0.74 10 ⁻⁴
3c-G1@GO-CC	2.30	0.95	41	0.84 10 ⁻⁴

[a] measures made in duplicate.

Biological tests on dendrons and GO functionalized with dendrons.

Some of us have shown previously that dendrimers bearing pyridine terminal functions, either free, or complexing copper were active in vitro against diverse cancerous cell lines [22]. It was shown that the most active compounds were the 3rd generation dendrimers bearing pyridine imine terminal functions, either free or complexing a metal (copper or gold). Thus, it seemed interesting to test all the small new dendrons synthesized as well as the corresponding materials.

The evaluation was carried out with the cancerous cell line HCT116 (human colon cancer). It should be noted that all compounds were soluble in stock solutions (10⁻² M in DMSO) but precipitated in the medium and on cells. The most active compounds were evaluated towards the non-cancerous RPE1 cells (Human retinal pigment epithelial-1), a non-transformed alternative to cancer cell lines. Experiments were carried out for 72 h, in triplicate, at two concentrations (10⁻⁵ and 10⁻⁶ M) in DMSO. The results shown in Table 1 indicate that the pyridine imine dendrons (2a-G1 and 3a-G1) are highly active at 10⁻⁵ M (not active at 10⁻⁶ M), and that the hydrazone pyridine dendrons (2c-G1 and 3c-G1) are not active against HCT116. It was shown in a previous work that third generation dendrimers bearing as terminal functions the same types of hydrazone pyridine functions than dendrons 2c-G1 and 3c-G1 were also non-active [22]. However, surprisingly, the most active dendrons are those functionalized with the dipyridine imine terminal functions (2b-G1 and 3b-G1). Indeed, these compounds are highly active at 10⁻⁵ M, and are the only ones still slightly active at 10⁻⁶ M.

In the next step, to verify the safety of the active compounds, they were tested towards the non-cancerous RPE1 cells, in the same conditions than with the HCT116 cell line. Deceptively, the dendrons are as toxic against the non-cancerous cells as against the cancerous cells (Table 2).

Table 2. Biological tests of dendrons in DMSO towards the cancerous cell line HCT116, and the non-cancerous cells RPE1.

Dendron	HCT116 cells ^[a]	HCT116 cells ^[a]	RPE1 cells ^[a]	RPE1 cells ^[a]
	% viability at 10 ⁻⁵ M ^[b]	% viability at 10 ⁻⁶ M ^[b]	% viability at 10 ⁻⁵ M ^[b]	% viability at 10 ⁻⁶ M ^[b]
2a-G1 ^[c,d]	0.6 (±0.2)	96.8 (±2.7)	0.2 (±0.2)	100.7 (±3.0)
2b-G1 ^[c,d]	1.8 (±0.7)	82.7 (±5.3)	0.9 (±0.1)	94.9 (±2.5)
2c-G1 ^[c]	99.8 (±3.8)	100.1 (±2.9)	-	-
3a-G1 ^[c,d]	4.2 (±0.4)	102.8 (±2.8)	3.1 (±2.4)	101.0 (±2.3)
3b-G1 ^[c,d]	9.8 (±0.2)	85.7 (±3.3)	3.1 (±1.6)	97.0 (±3.3)
3c-G1 ^[c,d]	95.5 (±2.1)	103.2 (±1.7)	-	-

[a] measures made in triplicate. [b] dendron concentration. [c] precipitated in medium. [d] precipitated on cells.

GO alone and the GO functionalized with the dendrons were tested in the same conditions. Tests were carried out from stock dispersions of the materials at 10⁻³ M in DMSO, but the materials precipitated in the medium and on cells. As shown in Table 3, GO alone is weakly toxic towards the cancerous HCT116 cells at 10⁻⁵ M. Graphene oxide functionalized with 2c-G1 and 3c-G1 is less toxic than GO alone, whereas 2b-G1@GO-N3 and 3a-G1@GO-CC are slightly more toxic. However, it is clear that there is no improvement offered by the grafting of dendrons to GO. In view of these results, these materials were not tested on non-cancerous cells.

Table 3. Biological tests of GO and GO functionalized with dendrons in DMSO towards the cancerous cell line HCT116.

Dendron grafted to GO	HCT116 cells[a]	HCT116 cells[a]
	% viability at 10 ⁻⁵ M[b]	% viability at 10 ⁻⁶ M[b]
GO	80.0 (±3.5)	102.1 (±3.4)
2a-G1@GO-N3[c,d, e]	82.1 (±2.9)	95.4 (±3.7)
2b-G1@GO-N3[c,d]	74.2 (±1.5)	92.1 (±2.9)
2c-G1@GO-N3[c,d]	94.7 (±2.4)	97.0 (±3.8)
3a-G1@GO-CC[c,d]	60.5 (±1.2)	96.2 (±2.7)
3b-G1@GO-CC[c,d]	92.5 (±1.4)	98.0 (±1.4)
3c-G1@GO-CC[c,d]	98.8 (±4.1)	101.3 (±2.3)

[a] measures made in triplicate. [b] material concentration. [c] precipitated in medium. [d] precipitated on cells. [e] dispersion in DMSO.

Conclusion

To summarize, we presented for the first time the grafting of phosphorhydrazone dendrons having either an azide or an alkyne on the core and diverse types of pyridine derivatives as terminal functions on GO functionalized with either alkyne or azide functions by the means of click chemistry. Grafting of dendrons having an alkyne at the core to GO functionalized with azides was the most efficient way. The synthesized hybrid materials have been investigated through FTIR, Raman Spectroscopy, and MAS-NMR analyses. The synthesized nanocomposites were tested subsequently against HCT116 cell lines, but deceptively only moderated activities have been obtained, probably due to their precipitation on cell lines. However, these hybrid nanomaterials could find other uses, for instance as catalysts in heterogeneous catalysis, after complexation of metal, in particular Cu by the pyridine-imine/hydrazone functions [17a].

Experimental Section

Essential Experimental Procedures/Data.

General strategy for the 3-step synthesis of the 2a-c-G1 family of dendrons. a) To a solution of the pentaaldehyde 1 (1.29 mmol, 1 g) and cesium carbonate (2.84 mmol, 0.92 g, in suspension) in THF (7 mL) was added dropwise a solution of 4-propargyloxyphenol 2 (1.42 mmol, 0.2 g) dissolved in THF (7 mL). The reaction mixture was stirred at 40 °C overnight. The salts were removed by centrifugation and the solution was concentrated under reduced pressure. The residue was then purified by column chromatography (DCM/ethyl acetate, 9.9/0.1 to 9.5/0.5, v/v). Product 2-G0 was recovered as a white powder in 43% yield. b) To a solution of 2-G0 (0.34 mmol, 0.3 g) in THF (5 mL) was added a solution of H₂NNMePSCI₂ in CHCl₃ (2.03 mmol, 7.5 mL). The reaction mixture was stirred overnight at room temperature. The solvent was removed under reduced pressure. The residue was then dissolved in a minimum amount of THF (4 mL) and precipitated in 100 mL of pentane/ether (4/1). The resulting powder was filtered and the procedure was repeated twice. Dendron 2-G1 was obtained as a white

powder in 89% yield. c) To a solution of 2-G1 (0.12 mmol, 0.2 g) and cesium carbonate (2.63 mmol, 0.86 g, in suspension) in THF (5 mL) was added dropwise a solution of phenol 5a (1.31 mmol, 0.28 g), 5b (1.31 mmol, 0.4 g), or 5c (1.31 mmol, 0.28 g) dissolved in THF (7 mL). The reaction mixture was stirred at 40 °C (5a) or room temperature (5b, 5c) overnight. The salts were removed by centrifugation and the clear solution was concentrated under reduced pressure. The residue was then dissolved in the minimum amount of THF (4 ml) and precipitated in 100 ml of pentane/ether (1/1), and washed with MeOH at 0 °C for 2b-G1. The resulting powder was filtered and the procedure repeated twice (precipitated with pentane at the end) to give the desired product as a white powder in 91% yield for 2a-G1, 62% yield for 2b-G1, and 83% yield for 2c-G1. The attribution of NMR signals is made according to Figure 8.

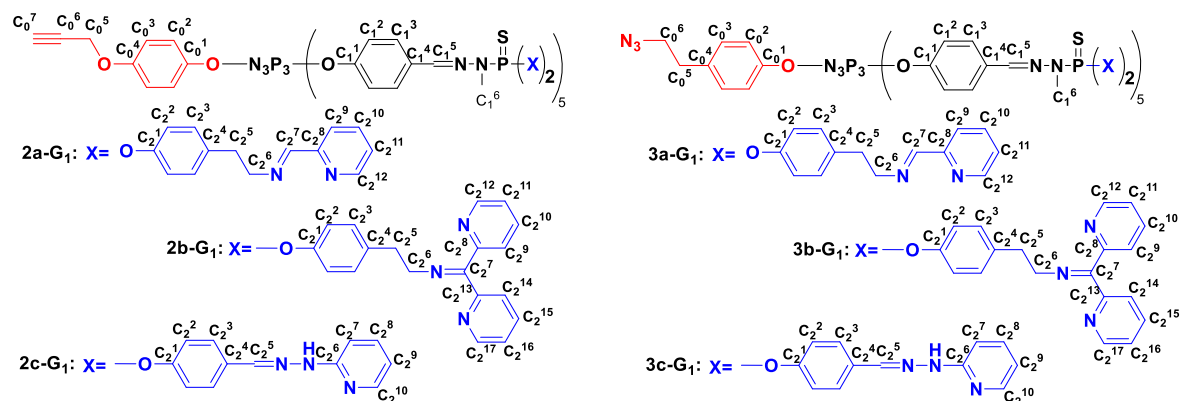


Figure 8. Numbering for NMR signals assignment.

2a-G1. $^{31}\text{P}\{^1\text{H}\}$ NMR (162 MHz, CDCl_3) δ 63.02 (s, P=S), 62.92 (s, P=S), 9.60 – 7.88 (m, P=N). ^1H NMR (400 MHz, CDCl_3) δ 8.66-8.58 (m, 20H, C_2^7, C_2^11), 8.02–7.99 (m, 10H, C_2^12), 7.61 – 7.46 (m, 35H, C_1^3, C_1^5, C_2^9, C_2^10), 7.11– 6.94 (m, 50H, C_1^2, C_2^3), 6.84 (d, J = 9.2 Hz, 2H, C_0^3), 6.70 (d, J = 9.2 Hz, 2H, C_0^2), 4.49 (s, 2H, C_0^5), 3.88 – 3.75 (m, 20H, C_2^6), 3.25 (d, J = 10.19 Hz, 6H, C_1^6), 3.19 (d, J = 10.19 Hz, 9H, C_1^6), 2.92 (m, 21H, C_2^5, C_0^7). ^{13}C { ^1H } NMR (101 MHz, CDCl_3) δ 159.7 (s, C_2^7), 151.38 – 151.10 (m, C_0^1, C_1^1), 150.4 (s, C_2^7, C_2^12), 149.09 (d, J = 7.2 Hz, C_2^1), 142.75 (s, C_2^8), 138.40 (s, C_1^5), 136.76 (s, C_2^4), 132.24 – 132.02 (m, C_0^4, C_1^4), 130.20 – 129.95 (m, C_0^3, C_2^3), 128.31 – 128.13 (m, C_1^3, C_2^10), 121.84 (s, C_2^9), 121.68 – 122.03 (m, C_1^2, C_2^2), 115.56 (s, C_0^2), 77.62 (s, C_0^7), 75.97 (s, C_0^6), 62.88 (s, C_2^6), 56.04 (s, C_0^5), 36.38 (s, C_2^5), 32.95 (d, J = 12.4 Hz, C_1^6).

2b-G1. $^{31}\text{P}\{^1\text{H}\}$ NMR (162 MHz, CDCl_3) δ 63.15 (s, P=S), 63.07 (s, P=S) 9.52 – 7.80 (m, P=N). ^1H NMR (400 MHz, CDCl_3) δ 8.64 (sbr, 10H, C_2^12), 8.47 (sbr, 10H, C_2^17), 8.04 (d, J = 8.0 Hz, 10H, C_2^14), 7.73 – 7.46 (m, 36H, C_1^3, C_1^6, C_2^10, C_2^15), 7.16 – 7.25 (m, 20H, C_2^11, C_2^16), 7.10 – 6.87 (m, 60H, C_1^2, C_2^2, C_2^3), 6.83 (d, J = 8.7 Hz, 2H, C_0^2), 6.67 (d, J = 8.7 Hz, 2H, C_0^3), 4.44 (s, 2H, C_0^5), 3.62 (sbr, 20H, C_2^6), 3.23 (d, J = 10.1 Hz, 6H, C_1^6), 3.16 (d, J = 10.1 Hz, 9H, C_1^6), 3.00 – 2.87 (m, 20H, C_2^5), 2.87 (s, 1H, C_0^7). ^{13}C { ^1H } NMR (101 MHz, CDCl_3) δ 167.14 (s, C_2^7), 156.79 (s, C_2^13), 155.26 (s, C_2^8), 154.81 (s, C_0^4), 151.33 (d, J = 5.0 Hz, C_1^1), 149.70 (s, C_2^12), 149.04 (s, C_2^1), 148.98 (s, C_2^17), 143.20 (s, C_0^1), 138.65 – 138.42 (m, C_1^5), 137.52 (s, C_2^4), 136.51 (s, C_2^10), 136.22 (s, C_2^15), 132.24 (s, C_1^4), 130.13 (s, C_2^3), 128.33 (s, C_1^3), 124.29 (s, C_2^16), 123.65 (s, C_2^9), 123.24 (s, C_2^11), 122.43 (s, C_2^14), 121.92 (s, C_1^2), 121.95 – 121.82 (m, C_2^2), 115.67 (s, C_0^2), 115.37 (s, C_0^3), 77.25 (s, C_0^7), 76.14 (s, C_0^6), 56.41 (s, C_0^5), 55.12 (s, C_2^6), 36.73 (s, C_2^5), 33.09 (dd, J = 12.7, 5.3 Hz, C_1^6).

2c-G1. $^{31}\text{P}\{^1\text{H}\}$ NMR (162 MHz, THF-d8) δ 60.47 (s, P=S), 7.05 – 6.58 (m, P=N). ^1H NMR (400 MHz, THF-d8) δ 9.85 (s, 10H, NH), 8.06 – 7.99 (m, 10H, C_2^10), 7.84 – 7.44 (m, 55H, C_1^3, C_1^5, C_2^2, C_2^5,

C₂⁸), 7.28 – 7.00 (m, 40H, C₁², C₂³, C₂⁷), 6.87 (d, J = 9.2 Hz, 2H, C₀³), 6.75 (d, J = 9.2 Hz, 2H, C₀²), 6.64 (m, 10H, C₂⁹), 4.58 (s, 2H, C₀⁵), 3.34 (d, J = 10.4 Hz, 6H, C₁⁶), 3.16 (d, J = 10.4 Hz, 9H, C₁⁶), 2.95 (s, 1H, C₀⁷). ¹³C {¹H} NMR (101 MHz, THF-d₈) δ 158.54 (s, C₂⁶), 156.16 (s, C₀⁴), 152.68 (s, C₁⁴), 151.93 (s, C₂⁴), 148.87 (s, C₂¹⁰), 143.56 (s, C₀¹), 138.30 (s, C₂², C₂⁸), 134.42 (s, C₂¹), 133.53 (d, J = 9.2 Hz, C₁¹), 129.29 (s, C₁⁵), 128.17 (s, C₂⁵), 122.81 – 122.27 (m, C₀³, C₁², C₁³, C₂³), 116.51 (s, C₀²), 115.93 (s, C₂⁹), 107.59 (s, C₂⁷), 77.34 (s, C₀⁶), 68.15 (s, C₀⁷), 56.58 (s, C₀⁵), 33.59 – 33.49 (m, C₁⁶).

General strategy for the 3-step synthesis of the 3a-c-G1 family of dendrons. a) To a solution of the pentaaldehyde 1 (0.64 mmol, 0.5 g) and cesium carbonate (1.51 mmol, 0.5 g, in suspension) in THF (7 mL) was added dropwise a solution of 4-(2-azidoethyl) phenol 3 (0.77 mmol, 0.11 g) dissolved in THF (7 mL). The reaction mixture was stirred at 40 °C overnight. The salts were removed by centrifugation and the solution was concentrated under reduced pressure. The residue was then purified by column chromatography (DCM/ethyl acetate, 9.9/0.1 to 9.5/0.5, v/v). Product 3-G0 was isolated in 78% yield as a white powder. b) To a solution of 3-G0 (1.69 mmol, 1.53 g) in THF (5 mL) was added a solution of H₂NNMePSCl₂ in CHCl₃ (9.32 mmol, 31.39 mL). The reaction mixture was stirred overnight at 40 °C. The solvent was removed under reduced pressure. The residue was then dissolved in a minimum amount of THF (4 mL) and precipitated in 100 mL of pentane/ether (4/1). The resulting powder was filtered and the procedure was repeated twice. Dendron 3-G1 was obtained in 56% as a white powder. c) To a solution of 3-G1 (0.18 mmol, 0.3 g) and cesium carbonate (3.86 mmol, 1.26 g, in suspension) in THF (5 mL) was added dropwise a solution of phenol 5a (1.98 mmol, 0.45 g), 5b (1.93 mmol, 0.59 g), or 5c (1.28 mmol, 0.27 g) dissolved in THF (7 mL). The reaction mixture was stirred at 40 °C overnight. The salts were removed by centrifugation and the clear solution was concentrated under reduced pressure. The residue was then dissolved in the minimum amount of THF (4 mL) and precipitated in 100 mL of pentane/ether (1/1), and washed with ethanol for 3b-G1. The resulting powder was filtered and the procedure repeated twice (precipitated with pentane at the end) to give the desired product as a white powder in 84% yield for 3a-G1, 62% yield for 3b-G1, and 72% yield for 3c-G1.

3a-G1. ³¹P{¹H} NMR (162 MHz, CDCl₃) δ 63.08 (s, P=S), 62.95 (s, P=S), 8.45 (s, P=N). ¹H NMR (400 MHz, CDCl₃) δ 8.76 – 8.57 (m, 20H, C₂⁷, C₂¹¹), 8.05 (s, 10H, C₂⁸), 7.67 – 7.43 (m, 35H, C₁³, C₁⁵, C₂⁹, C₂¹⁰), 7.18 – 6.86 (m, 54H, C₁², C₂², C₂³, C₀³, C₀²), 3.97 – 3.70 (m, 20H, C₂⁶), 3.33 – 3.26 (m, 8H, C₀⁶, C₁⁶), 3.21 (d, J = 9.9 Hz, 9H, C₁⁶), 2.95 (m, 20H, C₂⁵), 2.73 (t, J = 7.0 Hz, 2H, C₀⁵). ¹³C {¹H} NMR (101 MHz, CDCl₃) δ 159.73 (s, C₂⁷), 154.65 (s, C₂⁸), 151.44 – 151.37 (m, C₀¹, C₁¹), 150.40 (s, C₂¹²), 149.05 (d, J = 7.2 Hz, C₂¹), 138.37 (d, J = 14.01 Hz, C₁⁵), 136.78 (s, C₂⁴), 136.76 (s, C₂¹⁰), 136.78 (s, C₁⁴), 135.20 (s, C₀⁴), 130.08 (s, C₂³), 129.88 (s, C₀³), 128.24 (s, C₁³), 128.18 (s, C₂¹¹), 121.84 (s, C₁²), 121.37 (s, C₀²), 121.29 (s, C₂²), 120.25 (s, C₂⁹), 62.90 (s, C₂⁶), 52.12 (s, C₀⁶), 36.4 (s, C₂⁵), 34.47 (s, C₀⁵), 32.95 (d, J = 12.4 Hz, C₁⁶). IR (ATR) ν = 2100 (N₃) cm⁻¹.

3b-G1. ³¹P{¹H} NMR (162 MHz, CDCl₃) δ 63.16 (s, P=S), 63.03 (s, P=S), 8.37 (s, P=N). ¹H NMR (400 MHz, CDCl₃) δ 8.69 – 8.58 (m, 10H, C₂¹⁷), 8.50 – 8.42 (m, 10H, C₂¹⁷), 8.08 – 7.98 (d, 10H, C₂¹⁴), 7.73 – 7.48 (m, 36H, C₁³, C₁⁶, C₂¹⁰, C₂¹⁵), 7.24 – 7.16 (m, 20H, C₂¹¹, C₂¹⁶), 7.10 – 6.87 (m, 64H, C₀², C₀³, C₁², C₂², C₂³), 3.72 – 3.52 (m, 20H, C₂⁶), 3.27 – 3.22 (m, 8H, C₀⁶, C₁⁶), 3.16 (d, J = 10.17 Hz, 9H, C₁⁶), 3.00 – 2.87 (m, 20H, C₂⁵), 2.67 (t, J = 6.9 Hz, 2H, C₀⁵). ¹³C{¹H} NMR (101 MHz, CDCl₃) δ 167.04 (s, C₂⁷), 156.72 (s, C₂¹³), 155.18 (s, C₂⁸), 154.81 (s, C₀⁴), 151.34 – 151.27 (m, C₁¹), 149.58 (s, C₂¹²), 149.20 (s, C₂¹), 148.86 (s, C₂¹⁷), 143.20 (s, C₀¹), 138.62 – 138.40 (m, C₁⁵), 137.44 (s, C₂⁴), 136.37 (s, C₂¹⁰), 136.08 (s, C₂¹⁵), 132.19 (s, C₁⁴), 130.01 (s, C₂³), 128.17 (s, C₁³), 126.34 (s, C₀³), 125.24 (s, C₀²), 124.15 (s, C₂¹⁶), 123.53 (s, C₂⁹), 123.10 (s, C₂¹¹), 122.30 (s, C₂¹⁴), 121.15 (s,

C₁²), 121.95 – 121.87 (m, C₂²), 56.41 (s, C₀⁵), 55.12 (s, C₂⁶), 52.11 (s, C₀⁶), 36.63 (s, C₂⁵), 34.44 (s, C₀⁵), 33.09 (m, C₁⁶). IR (ATR) ν = 2100 (N₃) cm⁻¹.

3c-G1. 31P{1H} NMR (162 MHz, THF-d₈) δ 60.52 (s, P=S), 60.47 (s, P=S), 6.66 (s, P=N). 1H NMR (400 MHz, THF-d₈) δ 9.85 (s, 10H), 8.08 – 7.98 (m, 10H, C₂¹⁰), 7.82 – 7.48 (m, 55H, C₁³, C₁⁵, C₂², C₂⁵, C₂⁸), 7.28 – 7.00 (m, 42H, C₁², C₂³, C₂⁷, C₀³), 6.92 (d, J = 9.2 Hz, 2H, C₀²), 6.64 (m, 10H, C₂⁹), 3.32 (m, 17H, C₀⁶, C₁⁶), 2.72 (t, J = 7.1 Hz, 2H, C₀⁵). 13C{1H} NMR (101 MHz, THF-d₈) δ 158.53 (s, C₂⁶), 156.14 (s, C₀⁴), 152.64 (s, C₁⁴), 151.92 (s, C₂⁴), 148.85 (s, C₂¹⁰), 143.56 (s, C₀¹), 138.28 (s, C₂², C₂⁸), 134.38 (s, C₂¹), 133.51 (d, J = 9.2 Hz, C₁¹), 129.25 (s, C₁⁵), 128.28 (s, C₂⁵), 122.81 – 122.27 (m, C₀³, C₁², C₁³, C₂³), 116.49 (s, C₀²), 115.91 (s, C₂⁹), 107.49 (s, C₂⁷), 50.03 (s, C₀⁶), 32.38 (s, C₀⁵), 33.53 (m, [C]₁⁶). IR (ATR) ν = 2100 (N₃) cm⁻¹.

Synthesis of GO-N3. The synthesis was carried out by dispersing 100 mg of GO (1 mg/ml) and 80 mg of sodium azide in 100 ml of pure water under continuous stirring at 10 °C for 1 h. After lyophilizing the reaction mixture, the product was dispersed in 100 ml of water at 10 °C and purified by centrifugation with water (three times, 10000 rpm at 10 °C). The final product was isolated by lyophilization and stored at low temperature (-20 °C) until use.

GO-N3: IR (ATR) ν = 2100 (N₃) cm⁻¹. Anal. found: C, 44.50; H, 2.23; N, 1.19.

Two-step synthesis of GO-CC. a) Graphene oxide (50 mg) was treated with thionyl chloride (35 ml) in the presence of 0.5 ml of DMF in a 50 ml Schlenk flask at 70 °C under argon for 24 h. The excess of SOCl₂ was removed under reduced pressure, the functionalized graphene oxide was washed with THF, and filtered on a PVDF filter membrane. The procedure was repeated three times and the product GO-COCl was obtained as a black powder (too unstable to be characterized). b) The synthesis of the material GO-CC was carried out in DMF (60 ml) in the presence of modified graphene oxide GO-COCl, propargylamine (1 ml) and triethylamine (2 ml) at 50 °C. After centrifugation (three times, 10000 rpm at 10 °C) and lyophilization, GO-CC was obtained as a black powder.

GO-CC: IR (ATR) ν = 1712 (C=O), 1619 (N-C=O) cm⁻¹. Anal. found: C, 74.91; H, 2.39; N, 4.49.

General strategy for grafting dendrons 2a-c-G1 onto GO-N3: CuI (30 mg), DIPEA (0.5 ml) in DMF (5 ml) were placed in a Schlenk flask and stirred under argon. Once the reaction mixture became yellow, a solution of dendron 2a-c-G1 (100 mg) dissolved in DMF (10 ml) was added to the Schlenk and the reaction was stirred for an additional 30 minutes. A dispersion of GO-N3 (100 mg) in DMF (20 ml) was transferred to the Schlenk. The click reaction was performed by stirring the reaction at 40 °C for 72 hours. The solid was separated from the reaction mixture by filtration on a PVDF filter membrane and washed several times with THF, methanol, ethanol, and DCM, followed by vacuum drying. The materials 2a-c-G1@GO-N3 were recovered as a black powder.

2a-G1@GO-N3. 31P MAS NMR (162 MHz, rotor spinning rate 11 kHz) δ (61.8, P=S), (8.4, P=N). IR (ATR) ν = 2100 (N₃) cm⁻¹. Raman D (1340), G (1580) cm⁻¹. Anal. Calcd.: S, 2.23. Found: S, 1.69.

2b-G1@GO-N3. 31P MAS NMR (162 MHz, rotor spinning rate 20 kHz), δ (62.7, P=S), (8.4, P=N). IR (ATR) ν = 2100 (N₃) cm⁻¹. Raman D (1340), G (1580) cm⁻¹. Anal. Calcd.: S, 1.83. Found: S, 1.49.

2c-G1@GO-N3. 31P MAS NMR (162 MHz, rotor spinning rate 20 kHz), δ (62.5, P=S), (8.6, P=N). IR (ATR) ν = 2100 (N₃) cm⁻¹. Raman D (1340), G (1580) cm⁻¹. Anal. Calcd.: S, 2.31. Found: S, 2.30.

General strategy for grafting dendrons 3a-c-G1 onto GO-CC: 30 mg of CuI, 0.5 mL of DIPEA in 5 mL of DMF were placed in a Schlenk flask and stirred under argon. Once the reaction mixture became yellow,

a solution of modified graphene oxide GO-CC (100 mg) dispersed in 10 mL of DMF was added to the Schlenk and the reaction was stirred for an additional 30 minutes. A solution of dendron 3a-c-G1 (100 mg) in 20 mL of DMF was transferred to the Schlenk. The click reaction was performed by stirring the suspension at 40 °C for 72 hours. The solid was separated from the reaction mixture by filtration on a PVDF membrane and washed several times with THF, MeOH, ethanol, and DCM, followed by vacuum drying. The materials 3a-c-G1@GO-CC were recovered as a black powder.

3a-G1@GO-CC. 31P MAS NMR (162 MHz, rotor spinning rate 13.5 kHz), δ (62.7, P=S), (8.3, P=N). IR Disappearance of the azide band. Raman D (1340), G (1580) cm⁻¹. Anal. Calcd.: S, 2.22. Found: S, 1.66.

3b-G1@GO-CC. 31P MAS NMR (162 MHz, rotor spinning rate 13.5 kHz), δ (63.4, P=S), (8.3, P=N). IR Disappearance of the azide band. Raman D (1340), G (1580) cm⁻¹. Anal. Calcd.: S, 1.83. Found: S, 0.88.

3c-G1@GO-CC. 31P MAS NMR (162 MHz, rotor spinning rate 13.5 kHz), δ (62.7, P=S), (8.3, P=N). IR Disappearance of the azide band. Raman D (1340), G (1580) cm⁻¹. Anal. Calcd.: S, 2.30. Found: S, 0.96.

Biological tests. Cancer cell lines were obtained from the American type Culture Collection (ATCC, Rockville, MD) and were cultured according to the supplier's instructions. Briefly, human HCT-116 colorectal carcinoma cells were grown in Gibco McCoy's 5A supplemented with 10% fetal calf serum and 1% glutamine. Human hTERT-RPE1 cells were cultured in DMEM/F12 medium containing 10% fetal calf serum and 1% glutamine. Cell lines were maintained at 37 °C in a humidified atmosphere containing 5% CO₂. Cell viability was determined by a luminescent assay according to the manufacturer's instructions (Promega, Madison, WI, USA). Briefly, the cells were seeded in 96-well plates (2.5 × 10³ cells/well) containing 90 μ L of growth medium. After 24 h of culture, the cells were treated with the tested compounds at 1 and 10 μ M final concentrations. Control cells were treated with the vehicle. After 72 h of incubation, 100 μ L of CellTiter Glo Reagent was added for 15 min before recording luminescence with a spectrophotometric plate reader PolarStar Omega (BMG LabTech). The percent viability index was calculated from three experiments.

Acknowledgements

Thanks are due to the French-Moroccan program TOUBKAL (grant 41405WE to O.A.) the CNRS and UEMF for financial support.

References

- [1] H. C. Kolb, M. G. Finn, K. B. Sharpless, *Angew. Chem. Int. Ed.* 2001, 40, 2004-2021. *Angew. Chem.* 2001, 113, 2056-2075.
- [2] R. Huisgen, G. Szeimies, L. Moebius, *Chem. Ber.* 1967, 100, 2494-2507.
- [3] H. C. Kolb, K. B. Sharpless, *Drug Discov. Today* 2003, 8, 1128-1137.
- [4] J. Chen, B. Yao, C. Li, G. Shi, *Carbon* 2013, 64, 225-229.
- [5] H. Yang, Y. Kwon, T. Kwon, H. Lee, B. J. Kim, *Small* 2012, 8, 3161-3168.
- [6] a) Q. Tu, L. Zhao, X. Han, D. E. Wang, M. S. Yuan, C. Tian, J. Wang, *RSC Advances* 2016, 6, 95628-95632; b) W. Zheng, H. Li, W. Chen, J. Zhang, N. Wang, X. Guo, X. Jiang, *Small* 2018, 14, 1703857.
- [7] T. Wei, T. Dong, H. Xing, Y. Liu, Z. Dai, *Anal. Chem.* 2017, 89, 12237-12243.
- [8] K. C. Mei, N. Rubio, P. M. Costa, H. Kafa, V. Abbate, F. Festy, S. S. Bansal, R. C. Hider, K. T. Al-Jamal, *Chem. Commun.* 2015, 51, 14981-14984.

- [9] K. Sarkar, G. Madras, K. Chatterjee, *RSC Advances* 2015, 5, 50196-50211.
- [10] S. M. Grayson, J. M. J. Frechet, *Chem. Rev.* 2001, 101, 3819-3867.
- [11] D. A. Tomalia, *Soft Matter* 2010, 6, 456-474.
- [12] E. Apartsin, A. M. Caminade, *Chem. Eur. J.* 2021, 27, 17976-17998.
- [13] A. M. Caminade, C. O. Turrin, R. Laurent, A. Ouali, B. Delavaux-Nicot, *Dendrimers: Towards Catalytic, Material and Biomedical Uses*, Wiley, 2011.
- [14] a) N. Launay, A. M. Caminade, R. Lahana, J. P. Majoral, *Angew. Chem.-Int. Edit. Engl.* 1994, 33, 1589-1592. *Angew. Chem.* 1994, 106, 1682-1684; b) N. Launay, A. M. Caminade, J. P. Majoral, *J. Am. Chem. Soc.* 1995, 117, 3282-3283; c) M. Slany, M. Bardaji, A. M. Caminade, B. Chaudret, J. P. Majoral, *Inorg. Chem.* 1997, 36, 1939-1945.
- [15] A. M. Caminade, A. Ouali, R. Laurent, C. O. Turrin, J. P. Majoral, *Coord. Chem. Rev.* 2016, 308, 478-497.
- [16] a) C. Galliot, C. Larre, A. M. Caminade, J. P. Majoral, *Science* 1997, 277, 1981-1984; b) J.-P. Majoral, A. M. Caminade, *Eur. J. Inorg. Chem.* 2019, 1457-1475.
- [17] a) A. Ouali, R. Laurent, A. M. Caminade, J. P. Majoral, M. Taillefer, *J. Am. Chem. Soc.* 2006, 128, 15990-15991; b) M. Keller, V. Colliere, O. Reiser, A. M. Caminade, J. P. Majoral, A. Ouali, *Angew. Chem. Int. Ed.* 2013, 52, 3626-3629. *Angew. Chem.* 2013, 125, 3714-3717; c) P. Neumann, H. Dib, A. M. Caminade, E. Hey-Hawkins, *Angew. Chem. Int. Ed.* 2015, 54, 311-314. *Angew. Chem.* 2015, 127, 316-319; d) A.-M. Caminade, R. Laurent, *Coord. Chem. Rev.* 2019, 389, 59-72.
- [18] a) T. R. Krishna, M. Parent, M. H. V. Werts, L. Moreaux, S. Gmouh, S. Charpak, A. M. Caminade, J. P. Majoral, M. Blanchard-Desce, *Angew. Chem. Int. Ed.* 2006, 45, 4645-4648; *Angew. Chem.* 2006, 118, 4761-4764; b) F. Terenziani, V. Parthasarathy, A. Pla-Quintana, T. Maishal, A. M. Caminade, J. P. Majoral, M. Blanchard-Desce, *Angew. Chem. Int. Ed.* 2009, 48, 8691-8694; *Angew. Chem.* 2009, 121, 8847-8850; c) J. Qiu, A. Hameau, X. Shi, S. Mignani, J.-P. Majoral, A.-M. Caminade, *ChemPlusChem* 2019, 84, 1070-1080.
- [19] a) A. M. Caminade, J. P. Majoral, *Acc. Chem. Res.* 2004, 37, 341-348; b) D. H. Kim, P. Karan, P. Goring, J. Leclaire, A. M. Caminade, J. P. Majoral, U. Gosele, M. Steinhart, W. Knoll, *Small* 2005, 1, 99-102; c) T. D. Lazzara, K. H. A. Lau, A. I. Abou-Kandil, A. M. Caminade, J. P. Majoral, W. Knoll, *ACS Nano* 2010, 4, 3909-3920; d) W. Knoll, A. M. Caminade, K. Char, H. Duran, C. L. Feng, A. Gitsas, D. H. Kim, A. Lau, T. D. Lazzara, J. P. Majoral, M. Steinhart, B. Yameen, X. H. Zhong, *Small* 2011, 7, 1384-1391.
- [20] a) V. Le Berre, E. Trevisiol, A. Dagkessamanskaia, S. Sokol, A. M. Caminade, J. P. Majoral, B. Meunier, J. Francois, *Nucleic Acids Res.* 2003, 31, e88; b) J. P. Majoral, J. M. Francois, R. Fabre, A. Senescau, S. Mignani, A. M. Caminade, *Sci. China-Mater.* 2018, 61, 1454-1461.
- [21] a) L. Griffe, M. Poupot, P. Marchand, A. Maraval, C. O. Turrin, O. Rolland, P. Metivier, G. Bacquet, J. J. Fournie, A. M. Caminade, R. Poupot, J. P. Majoral, *Angew. Chem. Int. Ed.* 2007, 46, 2523-2526. *Angew. Chem.* 2007, 119, 2575-2578; b) M. Hayder, M. Poupot, M. Baron, D. Nigon, C. O. Turrin, A. M. Caminade, J. P. Majoral, R. A. Eisenberg, J. J. Fournie, A. Cantagrel, R. Poupot, J. L. Davignon, *Sci. Transl. Med.* 2011, 3, 11; c) E. Blattes, A. Vercellone, H. Eutamene, C. O. Turrin, V. Theodorou, J. P. Majoral, A. M. Caminade, J. Prandi, J. Nigou, G. Puzo, *Proc. Natl. Acad. Sci. U. S. A.* 2013, 110, 8795-8800; d) A. M. Caminade, S. Fruchon, C. O. Turrin, M. Poupot, A. Ouali, A. Maraval, M. Garzoni, M. Maly, V. Furer, V.

Kovalenko, J. P. Majoral, G. M. Pavan, R. Poupot, *Nat. Commun.* 2015, 6, 7722; e) A. M. Caminade, *Chem. Commun.* 2017, 53, 9830-9838.

[22] a) N. El Brahmī, S. El Kazzouli, S. M. Mignani, E. Essassi, G. Aubert, R. Laurent, A. M. Caminade, M. M. Bousmina, T. Cresteil, J. P. Majoral, *Mol. Pharm.* 2013, 10, 1459-1464; b) S. Mignani, N. El Brahmī, L. Eloy, J. Poupon, V. Nicolas, A. Steinmetz, S. El Kazzouli, M. M. Bousmina, M. Blanchard-Desce, A. M. Caminade, J. P. Majoral, T. Cresteil, *Eur. J. Med. Chem.* 2017, 132, 142-156.

[23] S. M. Mignani, N. El Brahmī, S. El Kazzouli, R. Laurent, S. Ladeira, A. M. Caminade, E. Pedziwiatr-Werbicka, E. M. Szewczyk, M. Bryszewska, M. M. Bousmina, T. Cresteil, J. P. Majoral, *Mol. Pharm.* 2017, 14, 4087-4097.

[24] L. Chen, S. Mignani, A. M. Caminade, J. P. Majoral, *Wiley Interdiscip. Rev. Nanomed. Nanobiotechnol.* 2019, 11, e1577.

[25] L. Chen, Y. Fan, J. Qiu, R. Laurent, J. Li, J. Bignon, S. Mignani, A. M. Caminade, X. Shi, J. P. Majoral, *Chem.-Eur. J.* 2020, 26, 5903-5910.

[26] Y. Chen, C. Tan, H. Zhang, L. Wang, *Chem. Soc. Rev.* 2015, 44, 2681-2701.

[27] a) A. Pramanik, S. Jones, Y. Gao, C. Sweet, A. Vangara, S. Begum, P. C. Ray, *Adv. Drug Delivery Rev.* 2018, 125, 21-35; b) E. Quagliarini, L. Digiacomio, D. Caputo, A. Coppola, H. Amenitsch, G. Caracciolo, D. Pozzi, *Nanomaterials* 2022, 12, 1397.

[28] Y. Y. Song, C. Li, X. Q. Yang, J. An, K. Cheng, Y. Xuan, X. M. Shi, M. J. Gao, X. L. Song, Y. D. Zhao, W. Chen, *J. Mater. Chem. B*, 2018, 6, 4808-4820.

[29] W. Jiang, J. Chen, C. Gong, Y. Wang, Y. Gao, Y. Yuan, *J. Nanobiotechnol.* 2020, 18, 50.

[30] a) A. M. Caminade, A. Hameau, J. P. Majoral, *Dalton Trans.* 2016, 45, 1810-1822; b) A. Zibarov, A. Oukhrib, J. Aujard Catot, C.-O. Turrin, A.-M. Caminade, *Molecules* 2021, 26, 4017.

[31] G. Franc, S. Mazerès, C. O. Turrin, L. Vendier, C. Duhayon, A. M. Caminade, J. P. Majoral, *J. Org. Chem.* 2007, 72, 8707-8715.

[32] a) M. Srinivasan, S. Sankararaman, H. Hopf, I. Dix, P. G. Jones, *J. Org. Chem.* 2001, 66, 4299-4303; b) E. Cavero, M. Zablocka, A. M. Caminade, J. P. Majoral, *Eur. J. Org. Chem.* 2010, 2759-2767.

[33] C. A. Grice, K. L. Tays, B. M. Savall, J. Wei, C. R. Butler, F. U. Axe, S. D. Bembenek, A. M. Fourie, P. J. Dunford, K. Lundeen, F. Coles, X. Xue, J. P. Riley, K. N. Williams, L. Karlsson, J. P. Edwards, *J. Med. Chem.* 2008, 51, 4150-4169.

[34] A. Makarem, K. D. Klika, G. Litau, Y. Remde, K. Kopka, *J. Org. Chem.* 2019, 84, 7501-7508.

[35] D. Riegert, A. Pla-Quintana, S. Fuchs, R. Laurent, C. O. Turrin, C. Duhayon, J. P. Majoral, A. Chaumonnot, A. M. Caminade, *Eur. J. Org. Chem.* 2013, 2013, 5414-5422.

[36] E. R. de Jong, N. Deloch, W. Knoll, C. O. Turrin, J. P. Majoral, A. M. Caminade, I. Koper, *New J. Chem.* 2015, 39, 7194-7205.

[37] Q. Vanbellinghen, P. Servin, A. Coinaud, S. Mallet-Ladeira, R. Laurent, A. M. Caminade, *Molecules* 2021, 26, 2333.

[38] W. S. Hummers, R. E. Offeman, *J. Am. Chem. Soc.* 1958, 80, 1339-1339.

[39] J. I. Paredes, S. Villar-Rodil, A. Martínez-Alonso, J. M. D. Tascón, *Langmuir* 2008, 24, 10560-10564.

[40] S. Eigler, Y. Hu, Y. Ishii, A. Hirsch, *Nanoscale* 2013, 5, 12136-12139.

[41] a) M. M. Lucchese, F. Stavale, E. H. M. Ferreira, C. Vilani, M. V. O. Moutinho, R. B. Capaz, C. A. Achete, A. Jorio, *Carbon* 2010, 48, 1592-1597; b) S. Eigler, A. Hirsch, *Angew. Chem. Int. Ed.* 2014, 53, 7720-7738. *Angew. Chem.* 2014, 126, 7852-7872.

[42] a few selected publications: a) M. R. Attwood, B. S. Brown, R. M. Dunsdon, D. N. Hurst, P. S. Jones, P. B. Kay, *Bioorg. Med. Chem. Lett.* 1992, 2, 229-234; b) S. Sato, M. Tetsuhashi, K. Sekine, H. Miyachi, M. Naito, Y. Hashimoto, H. Aoyama, *Bioorg. Med. Chem.* 2008, 16, 4685-4698; c) Y. Zheng, W. B. Song, L. J. Xuan, *Tetrahedron* 2016, 72, 5047-5050.